JACS
JOURNAL OF THE AMERICAN CHEMICAL SOCIETY

ARTICLE

pubs.acs.org/JACS

Dynamics on the Electronically Excited State Surface of the Bioluminescent Firefly Luciferase−Oxyluciferin System

Chang-ik Song and Young Min Rhee*

Institute of Theoretical and Computational Chemistry and Department of Chemistry, Pohang University of Science and Technology (POSTECH), Pohang, 790-784 Korea

Supporting Information

ABSTRACT: Dynamics of the firefly luciferase−oxyluciferin complex in its electronic ground and excited states are studied using various theoretical approaches. By mimicking the physiological conditions with realistic models of the chromophore oxyluciferin, the enzyme luciferase, and solvating water molecules and by performing real time simulations with a molecular dynamics technique on the model surfaces, we reveal that the local chromophore-surrounding interaction patterns differ rather severely in the two states. Because of the presence of protein, the solvation dynamics of water around the chromophore is also peculiar and shows widely different time scales on the two terminal oxygen atoms. In addition, simulations of the emission with the quantum-mechanics/molecular-mechanics approach show a close relationship between the emission color variation and the environmental dynamics, mostly through electrostatic effects from the chromophore-surrounding interaction. We also discuss the importance of considering the time scales of the luminescence and the dynamics of the interaction.

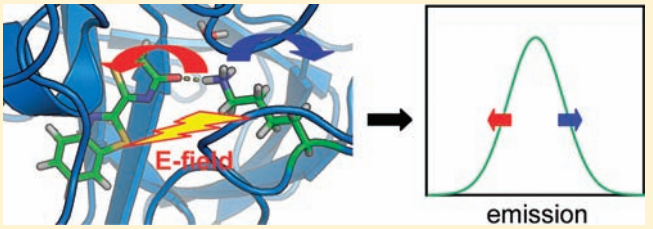

1. INTRODUCTION

Bioluminescence is one of the most fascinating natural phenomena whose purpose spans a variety of usages, including communication, appealing to prey, and disguising in insects and fish.[1] Among various creatures, bioluminescence from fireflies has gained much interest for its diverse spectral distributions by different species[2] from green to red, together with surprisingly high quantum yield.[3] The color variation is especially interesting as different colors are generated from a single luciferin species. In fireflies, the light emission is realized by the enzyme luciferase whose active site has a place for luciferin to react with Mg-ATP and, in turn, be oxidized to electronically excited oxyluciferin.[4] There have been many suggestions meant to improve our understanding of the fundamental chemistry of color modulation for several decades, including keto−enol equilibrium,[5] microenvironment of the luciferase−oxyluciferin complex,[6] twisted intramolecular charge transfer,[7] and resonance structure.[8] However, the exact mechanism has been a puzzle for many researchers for decades.

In fact, one of the most informative results appeared recently with X-ray structures of luciferase−oxyluciferin complexes with varying protein−ligand interaction patterns, up to a resolution of 1.30 Å.[9] The investigators also proposed that different geometrical relaxations involved with different mutants are related to the color modulation effect. Paired with the variety of practical applicabilities such as in vivo imaging[10] and photodynamic therapy,[11] this new finding apparently has reignited the interest in the firefly bioluminescence and its color modulation in the past few years.[12] However, a consensus about the detailed aspect of the involved chemistry is yet to be reached.

One of the important puzzles to resolve is the exact identity of the emitting molecule. After some debate,[13] it is now widely accepted that the phenolate form of the benzothiazole moiety (deprotonated O_{6r} on the six-membered ring in Scheme 1) is appropriate[12d,f,g,14] because of its increased acidity[15] in the excited state. Moreover, it is shown that upon protonation into the neutral form, it will have a deep blue transition instead of green or red.[14a] In addition, the deprotonation is suggested to have crucial effects on lowering the activation barrier of dioxetanone to oxyluciferin conversion and on the related charge-transfer-induced luminescence (CTIL).[16] On the contrary, the chemical nature of the thiazole ring is still being vigorously debated, even many years after Shimomura and co-workers' experimental confirmation about the nascent keto generation from dioxetanone.[17] Branchini et al. demonstrated that this keto species with an unprotonated oxygen on the thiazole ring (O_{5r} on the five-membered ring in Scheme 1) can emit in various colors, based on experiments with 5,5-dimethyloxyluciferin.[18] On the basis of ab initio and semiempirical calculations, Orlova et al. have pointed out the possibilities of in vivo enol formation from the keto form on this thiazole moiety and have proposed that emission of light from the enol form is plausible but not mandatory in explaining the color variation.[19] Various isomers and tautomers were then calculated by time-dependent density functional theory (TDDFT) with continuum solvent models.[20] For a thorough review of the theoretical accounts of the various

Received: February 25, 2011
Published: July 05, 2011

Scheme 1. Suggested Mechanism of Excited Oxyluciferin Generation

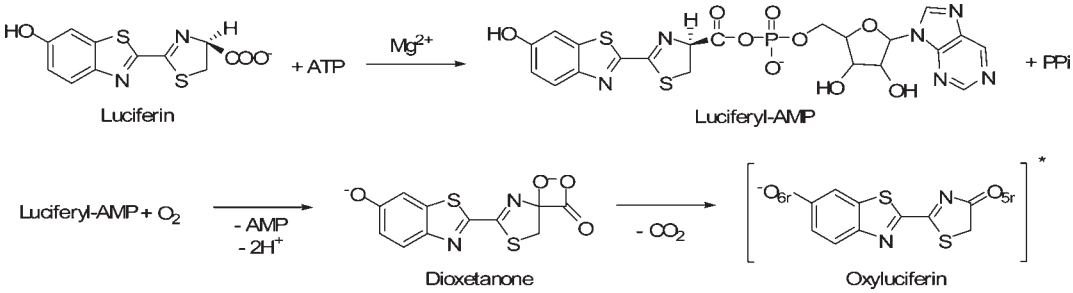

potential light emitters, readers are referred to a recent review by Esteves da Silva and co-workers.[12i]

At least it appears that there is no doubt about the nascent keto generation.[17] In fact, this idea of nascent keto generation was also supported by a high-level ab initio calculation on the chemical mechanism of the transformation from dioxetanone to excited state oxyluciferin, by considering topologies of transition state and conical intersection of dioxetanone.[12g] Also, Liu et al. agreed on this idea by studying the underlying detailed mechanism of the chemiluminescent decomposition of dioxetanone.[21] In a subsequent study, Chen et al. further suggested that this keto species is responsible for the light emission in the firefly luciferase.[14b] Recently, however, Naumov et al. have proposed the enol form as the emitter, based on similarities between crystal structure of pure oxyluciferin and structural data of the protein—emitter analogue complex with regard to the interaction patterns with proximate protein residues and other cofactors.[14a] In addition, they reconfirmed this in vivo enol hypothesis based on their pH titration experiments, proposing that the intermolecular factors, including hydrogen bonds, Coulombic interactions, and neighboring $\pi-\pi$ stacking, could determine the emitter chemical form and the emission color. Much of the apparent mutual contradiction between these recent propositions would be avoided only if the nascent ketone can convert into enol under physiological conditions within the lifetime of the electronically excited ketone (1—10 ns).[12f,22]

In this article, we present a theoretical study of the oxyluciferin bound to the luciferase in solution so that it mimics the actual physiological emitting condition[23] in the electronic excited state. While previous theoretical studies have mainly focused on static pictures with quantum chemical approaches, we concentrate on the dynamic features of the oxyluciferin—luciferase complex. Indeed, to the best of our knowledge, dynamic information obtained in a statistically meaningful way with a reliable model for the excited state has not been reported for firefly bioluminescence. Such an approach is important in obtaining new information that may not be easily accessed from experiments because of limitations at spatial or temporal resolutions with atomic details. With the combination of molecular dynamics (MD) and quantum-mechanics/molecular-mechanics (QM/MM) methods on both electronic ground and excited state surfaces, we show that the nearby structures around the oxyluciferin are quite different in the two electronic states. This difference, which occurs mainly because of the charge-transfer character of the electronic transition, leads to markedly different water mobility on the two main hydration sites on the oxyluciferin when it is bound in the protein. We also show that a protonated residue, not water molecules, participates importantly in stabilizing the nascent keto group in the excited state. At first glance, the interaction from a protonated species may appear to open a catalytic route for an efficient transform of keto into enol. However, after considering the reaction energetics, we show this proton transfer is an implausible conversion pathway. Because the keto—enol tautomerization within the lifetime of the excited state of oxyluciferin can be attained only by a catalytic proton transfer, our findings support the keto hypothesis and suggest the nascent keto will be the emitting species. We finally show that neighboring interaction with the structurally fluctuating protein residues around oxyluciferin can actually modulate the emission color to a large extent and conclude that the wide emission range from green to red can still be covered only with the keto species. With these, we suggest the importance of considering the dynamical features in the actual excited state for firefly bioluminescence. It is likely that this aspect will generally apply to other biological systems involving charge-transfer electronic transitions.

2. METHODS

Molecular dynamics (MD) simulations have been performed with GROMACS version 4.0[24] with the double-precision representation of floating point numbers. The system consists of oxyluciferin (OLU^-),[25] AMP, luciferase, and 30409 TIP3P water molecules. Initial geometries of OLU^-, AMP, and surrounding luciferase were extracted from the X-ray structural data[9] together with two additional Na^+ counterions for charge neutrality. Because a keto species is the nascently generated molecule in the protein,[17] for simulations, one may assume either neutral OLU (protonated O_{6r}) or anionic OLU^- (deprotonated O_{6r}). On the basis of the experimental[14a] and theoretical[14b] evidence that the neutral species will emit in deep blue, we will adopt only the anionic form in this work. It is also noted that even if the neutral form is somehow generated in the beginning, deprotonation will be predominant in the excited state because of the increased acidity[15] and the ultrafast proton transfer to solvent similar to the features of other phenol-like molecules.[14a,15b] In a later section, we will show that water resolvation on the O_{6r} side is also very fast, which will surely facilitate the deprotonation process.

The simulation system was generated by soaking the molecules into a pre-equilibrated box of water. The initial side length of the cubic simulation box was 100 Å. The force field parameters for the OLU^- in the ground and excited states were adopted from our previous result.[26] The OLU^- model includes electrostatic and dispersive interaction parameters together with a torsional barrier potential against thiazole—benzothiazole twisting, fully obtained with quantum chemical data. Internal vibrations were adjusted on the basis of harmonic models. Even though the parameter validation is not feasible because of the lack of experimental data for OLU^- itself, the same approach could be successfully applied to studying the resolvation dynamics after the charge-transfer transition in coumarin 153.[27] Even though the harmonic model

may become unreliable in reproducing short time dynamics involving chromophore vibrational relaxations,[27] this aspect will not be important in describing the dynamics of the chromophore−water and chromophore−protein interactions. The model for AMP was adapted from Amber ATP[28] by modifying parameters on the two phosphate groups for proper molecular charge. Parameters for all the other residues were from the OPLS force field.[29] The initial conformation was stabilized first by performing steepest descent energy minimization steps followed by 1 ns of a randomizing short MD run. Starting from this structure, we performed an additional 10 ns simulation as a production run. A total of 100 such trajectories were obtained. Obtaining each trajectory took approximately 12 days of CPU time when eight cores were used in parallel with two Intel X5560 (2.8 GHz) processors. The simulation length was similarly chosen to be the lifetime of the excited state, mainly because we are interested in dynamics that can take place within this time window. In the OLU−luciferase case, where the excited state is generated by chemical reaction rather than by light absorption at equilibrium as in other fluorescent proteins, following the more stringent choice of initial conditions versus the approach described above is impractical. As long as the overall protein structure with the excited OLU^- is not excessively different from the X-ray structure, initial condition-related artifacts especially with the water content can be avoided by considering various initial conditions, which will be explained in the next section. Because we are monitoring the dynamics over a 10 ns period with multiple trajectories together with carefully modeled OLU potential energy surfaces, any structural changes over the luminescence lifetime such as OLU reorientation or cis−trans isomerization can be recognized during the simulations. In fact, no such events were registered in any trajectory.

Simulations were performed on both the ground and excited state potential energy surfaces. The ground and excited state simulations will of course denote the calculations with the ground and the excited state OLU^- parameters, respectively. To elucidate the effect of water molecules neighboring OLU^-, two additional sets of MD trajectories were simulated. The first one involved a system generated by removing the two closest water molecules from the benzothiazole oxygen (O_{6r}). The other one was generated by removing the two closest water molecules from the thiazole oxygen (O_{5r}). Thus, six sets of MD runs were performed in total by utilizing ~160 years of aggregate CPU time on a supercomputer cluster. Constant-temperature and constant-pressure (NPT) molecular dynamics protocols were adopted following Berendsen's weak coupling algorithms,[30] together with three-dimensional periodic boundary conditions. Electrostatic and Lennard-Jones interactions were considered with 12 Å cutoffs with 10 Å tapers. Nonbonded neighbor lists were updated every 10 steps of MD, and the integration step size was 2 fs. All bonds involving hydrogen atoms were constrained with the LINCS algorithm.[31]

QM/MM calculations were conducted with Q-Chem version 3.2 (developers' version)[32] interfaced with CHARMM.[33] The geometries for the QM/MM single-point energy calculations or optimizations were obtained from the MD trajectories described above. The QM region is defined as the active site containing OLU^- and a few additional residues and/or water molecules, which will be explained on a case-by-case basis below. The MM region of course contains the remainder of the system. The constrained optimizations for considering the possibility of the proton-transfer reaction were performed on the excited state surface with QM regions defined with OLU^-, a proton-donating amino acid side chain, and one nearby water molecule. The geometries were obtained at the level of configuration interaction singles (CIS)[34] with the 6-31G(d) basis set, and then the energies were corrected with second-order perturbation, through the RI-CIS(D) method.[35] This includes the effect of the dynamical electron correlation on the energy surface description. The effect of the static correlation was additionally considered through the use of the state-averaged complete active space self-consistent field method (SA-CASSCF).[36] Details of the adopted CASSCF scheme are described in a later part of this section.

The OLU^- emission energy calculations within the enzyme were conducted by including OLU^- as the only QM region, at the level of RI-CIS(D) with the 6-311G(d,p) basis set. Using TDDFT with conventional exchange-correlation functionals sometimes yielded spuriously low-energy states, which is likely related to the issue involved with charge-transfer transitions.[35b,37] Even though RI-CIS(D) tends to underestimate the S_0-S_1 gap to some degree for OLU^- when compared to the more reliable EOM-CCSD results, the trend with which the gap changes depending on the OLU^- geometry and environment is well-preserved. Therefore, we applied EOM-CCSD corrections[38] as

$$E = E_{QM/MM}[\text{RI-CIS(D)}/bb] + E_{gas}[\text{EOM-CCSD}/sb] - E_{gas}[\text{RI-CIS(D)}/sb]$$

for the excited state energies. Here, bb denotes a bigger basis set, which is 6-311G(d,p) in this work, and sb a smaller set, 6-31+G(d). The two subscripts, QM/MM and gas, of course represent results from QM/MM style and gas phase calculations, respectively. With equivalent corrections for the ground state energies with RI-MP2 and CCSD results, S_0-S_1 gap corrections can be obtained in a manner similar to Pople's correction schemes.[38b] The use of a diffuse basis set, 6-311+G(d,p), in place of the 6-311G(d,p) basis set on a small number of randomly selected conformations had a negligible effect on the emission energies, and therefore, the 6-311G(d,p) basis set was adopted for efficient evaluations during the production calculations.

The interactions between the QM and MM regions were expressed by the additive approach, and the additional link atom was included when needed.[39] The nonbonded interactions within the MM region were considered with the same cutoff criteria. The MM particles were treated as point particles to QM region, and the electrostatic interactions with MM point particles were calculated by considering the electron distribution generated by the relaxed one-particle density matrices.[34]

In the calculation of the proton affinity of OLU^- in the excited state, geometries of the protonated and unprotonated species were obtained with SA-CASSCF[36] with the ANO-RCC-VDZP basis set,[40] followed by multistate second-order perturbative (MS-CASPT2) energy corrections.[41] The selected active space was "8 electrons in 8 orbitals", following the suggestion by Yang and Goddard.[42] Each of the CASPT2 calculations was performed on the basis of the zeroth-order Hamiltonian defined as a sum of one-electron effective Fock operators[43] together with a 0.25 au level shift to avoid intruder state problems.[44] These multireference calculations were performed with MOLPRO.[45] For dynamic correlations, orbital spaces that were maximally allowed by the program for CASPT2 were considered, leaving 36 core orbitals uncorrelated.

In various places, we needed to consider the appearances of hydrogen bonds from molecular dynamics trajectory snapshots. A hydrogen bond was registered if a structure exhibited a hydrogen donor−acceptor (D−A) distance shorter than 2.8 Å and a D−H−A angle larger than 150°.

3. RESULTS AND DISCUSSION

Water Distributions around Two Oxygen Atoms in Oxyluciferin. The cavity in which the deprotonated oxyluciferin (OLU^-), the chromophore, is located is naturally very different from the aqueous environment. In fact, when there is lack of solvating water around the chromophore, the luminescence environment from the protein-bound system can even be closer to the gas phase situation rather than to the aqueous solution. We have previously shown that resolvation around OLU^- in the bulk aqueous phase occurs within a few picoseconds,[26] with decreasing water density around the benzothiazole oxygen (O_{6r}) and increasing density around the thiazole oxygen (O_{5r}) on the S_1

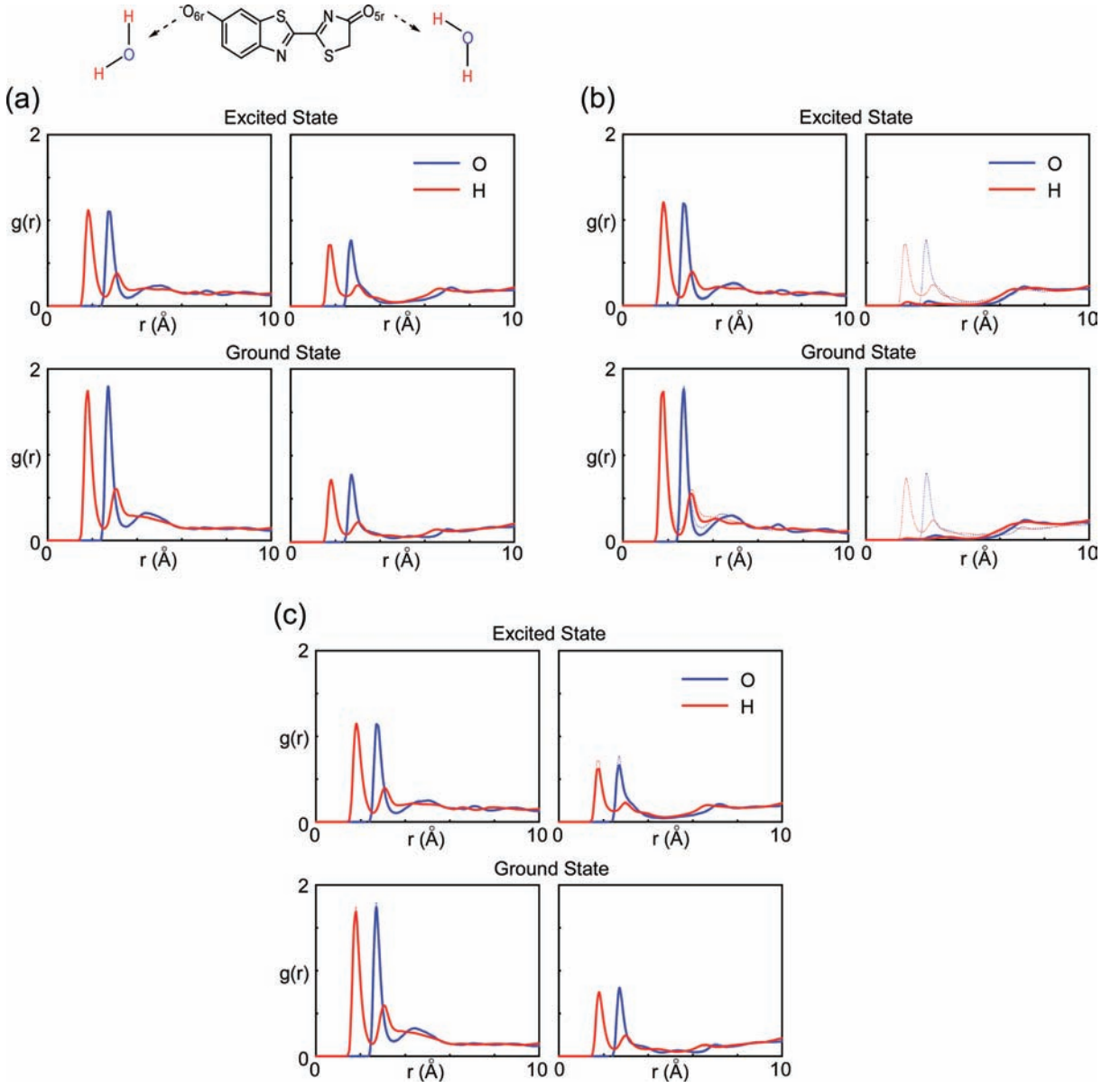

Figure 1. Solvent distribution functions around O_{6r} (left) and O_{5r} (right) obtained with ground state and excited state simulations of oxyluciferin in luciferase. The distributions were generated with trajectories initiated (a) from fully hydrated structures, (b) after the removal of two nearby water molecules around O_{5r}, and (c) after the removal of two water molecules around O_{6r}. Results from panel a are overlaid as dotted lines in panels b and c for the sake of comparison.

surface compared to the S_0 surface. This solvation difference is induced by the charge-transfer character of the S_1 state of OLU^-, with a larger negative charge concentrated on O_{5r} in this state.

To see the relevant time scale in the luciferase-bound case, we have calculated the solvent distribution function around the two oxygen atoms of OLU^- in the same manner. When the trajectories on S_0 and S_1 surfaces were initiated after full hydration (by locating water molecules at the positions found in the crystal structure[9] plus complete soaking), the first solvation shell structure around O_{6r} shows a behavior similar to that in the aqueous case with an ~30% decrease in the peak height in the S_1 case (Figure 1a). However, the solvation structure around O_{5r} does not exhibit such a behavior: it is similar on both S_0 and S_1 surfaces with the protein, while it is markedly different in the bulk water (~65% increase in the peak height on S_1).[26] This suggests that the resolvation dynamics around O_{5r} is much slower than in the bulk phase, beyond the simulation time scale (~10 ns). Because the excited state lifetime (1−10 ns)[12f,22] is close to our simulation time, this signifies that the water structure will not have enough time to re-equilibrate upon the generation of OLU^- through the enzymatic reaction. To further verify this proposition, we have again calculated the solvent distribution by running the same simulations of the two modified sets. (As explained in the previous section, the first additional set is started after the removal of two nearby water molecules around O_{5r}, and the second is started after the removal of two nearby water molecules around O_{6r}.) Upon removal of two water molecules around O_{5r} (Figure 1b), resolvation indeed does not occur within the simulation time. However, around O_{6r}, resolvation is completed within the same simulation time (Figure 1c). In fact, the solvent

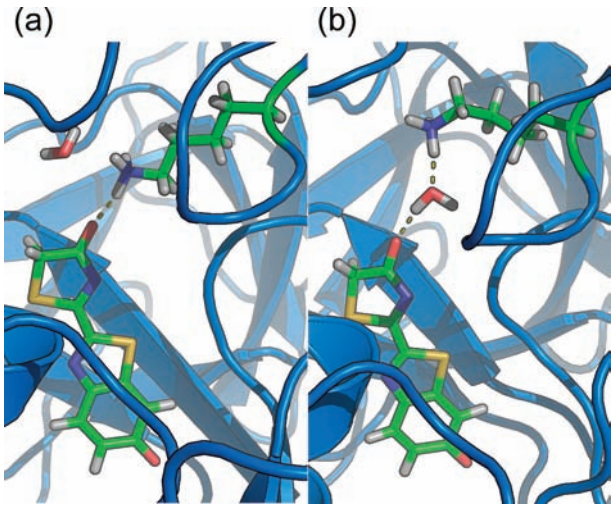

Figure 2. Very often in the excited state, oxyluciferin forms a hydrogen-bonding ion pair with Lys531 either directly or through water mediation. Representative structures of the (a) direct and (b) bridged ion pairs.

distributions with different starting water contents around O_{6r} converge to the same result well within the 1 ns as under the aqueous condition.[26]

From this figure, we can infer that the benzothiazole moiety (O_{6r} side) is practically more exposed to the bulk water than the thiazole moiety (O_{5r} side). In some sense, this is surprising, as a visual inspection of the crystal structure actually shows degrees of exposure on the two sides that are not too different. Within 3 Å spheres centered at O_{5r} and O_{6r}, ~40 and ~60 $Å^3$ of empty space exist, respectively. Even when different criteria were adopted for the calculation of the degree of exposure, the ratio between the two volumes remains similar. (See the Supporting Information and Table S1 for a detailed description of this quantitative comparison of the degree of exposure.) However, water responds promptly on the O_{6r} side to the charge migration upon the generation of the excited OLU^- and its deexcitation. The less exposed O_{5r} side will not experience stabilization through such resolvation. This finding actually suggests an important precaution in using the experimentally determined structure: the structure around this atom should be inferred from the nascent state right after the generation of the excited OLU^- (OLU^{-*}) rather than from the crystal structure with the ground state OLU^- or its analogue. This is also important as the O_{5r} side is the part where the precursor of the luminophore experiences the largest structural change along the chemical reaction path. As shown in Scheme 1, the thiazole moiety is bulkier with directly attached carboxylic or dioxetanone groups before the generation of OLU^{-*}, and there may be fewer water molecules around it under the physiological condition than considered in various previous studies.

Stabilizing Factors around the Thiazole Oxygen. As described above, we have shown that the resolvation around O_{5r} is much slower than the luminescence lifetime and suggested a possibility that there may be fewer than the optimal number of water molecules around this atom under the physiological condition. Therefore, the solvation by water may not be sufficient to stabilize the relatively large negative charge on O_{5r}. Rather, water molecules should be considered as additional "movable residues" that compete with other protein residues for the interaction with OLU^{-*}. In fact, it is easy to imagine that the large partial negative charge on O_{5r} will seek Coulombic interactions with positively charged ionic groups. Such ionic attractions always become important whenever ions are not effectively solvated and are exposed as bare charges.

Table 1. Fractions of Snapshots Showing Different Types of Lys531−OLU^- Interactions Obtained with Trajectories Initiated from Fully Hydrated Structures

type	S_0 simulation	S_1 simulation
bridged	8.7%	5.6%
direct	6.2%	47.9%
none	85.1%	46.5%

From our simulations, it is observed that the Lys531 residue, which will exist in a protonated and positively charged state under the physiological condition (pH ~7), is indeed often located near the thiazole ring moiety and exerts a stabilizing effect on O_{5r}. When all the trajectories were inspected carefully, two distinctive patterns of ion pair formation between OLU^{-*} and Lys531 were registered. One is a "direct form" in which the ammonium group on Lys531 is directly attached to O_{5r} through hydrogen bonding, and the other is a "bridged form" in which the contact is mediated by a water molecule (Figure 2). The fractions of trajectory snapshots with such formations are listed in Table 1. In fact, the patterns of the neighboring group interaction on the ground and excited state surfaces are significantly different. When the trajectories were initiated from the fully hydrated structure, ~40% more direct ion pair formation was observed on the excited surface than on the ground state. A similar trend is found with the trajectories initiated after the removal of nearby water molecules around O_{5r} and O_{6r}. Thus, we can clearly manifest that direct ion pair formation is strongly promoted for the excited state OLU^-, regardless of the nearby water structure. What is more important will be the time scale for these ion pair formations. To elucidate how fast the Lys531 chain can migrate toward OLU^{-*} on average, we have also plotted the growth of these populations in Figure 3. Within the lifetime of the excited state, namely, well before the deexcitation of OLU^{-*}, the ionic contact forms with Lys531. This time scale of ion pair formation (~1 ns) compares interestingly with the time scales of water motion: the resolvation on O_{6r} occurs much faster than 1 ns, while the same dynamics on O_{5r} occurs much slower than this time. As explained previously, the solvent-accessible free volumes around O_{5r} and O_{6r} are rather similar, but the time scales of water motion are at least 1 order of magnitude different. In fact, we believe this time scale difference is induced by a competition for water among different highly hydrophilic groups around O_{5r} (OLU^{-*}, Lys531, and AMP) and then amplified by the spatial confinement. When such ionic groups are closely located in a rather confined region with blocked bulk water flow, detaching a water molecule that is stuck on one group will demand a relatively high free energy. From the behavior on O_{6r}, we can see that the confinement alone cannot induce a similar deceleration in water motion.

On the basis of the fact that this strong tendency for ion pair formation on O_{5r} is induced by the increased negative charge in the excited state, we can infer that O_{5r} may even have high basicity. In fact, multireference ab initio calculations predict a stronger proton affinity of O_{5r} than O_{6r}: the excited state geometry-optimized OLUH* (Scheme 2),[46] which has the proton attached to O_{5r},[47] is lower in energy than the HOLU* species

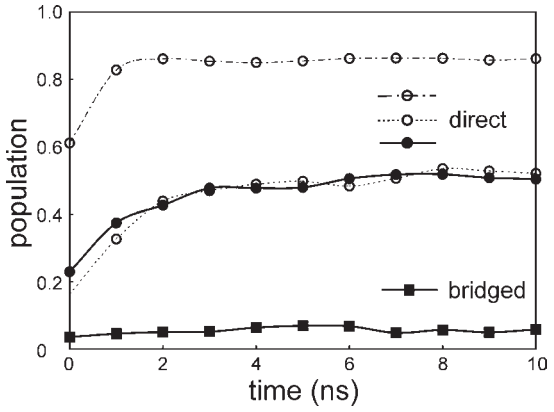

Figure 3. Population growth of the Lys531−OLU^- ion pairs as a function of time. For the direct pair, three different results from the trajectories were initiated with fully hydrated initial structure (—), with two fewer water molecules around O_{6r} (···), and with two fewer molecules around O_{5r} (---) are shown. Values on each time point were obtained by averaging the preceding 1 ns simulation results based on conformations recorded at 10 ps intervals. Time zero values denote the averages from the randomizing 1 ns simulations. See Figure S3 of the Supporting Information for results without averaging.

Scheme 2. Two Protonated Forms of Excited State Oxyluciferin

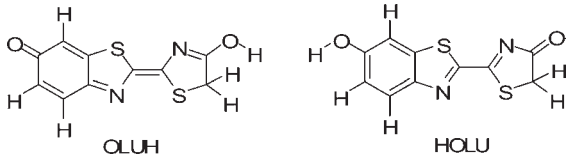

(Scheme 2), where the additional proton is used to neutralize the phenolate group. The energy difference in the two protonated species $[E(\mathrm{HOLU}^*) - E(\mathrm{OLUH}^*)]$ was found to be 4.1 kcal/mol. Compared to the ground electronic state, where HOLU is more stable $[E(\mathrm{HOLU}) - E(\mathrm{OLUH}) = -34.8$ kcal/mol] within the same method, this energy difference is in fact significant. This also explains the strong tendency of OLU^{-*} to seek a neutralizing effect on O_{5r} by dragging a neighboring positively charged residue, Lys531. Again, we stress that the tendency is more pronounced in the excited state, and the ground state structural information will not reveal this. In fact, the distribution of the distances between O_{5r} and the terminal N atom in Lys531, obtained from the ground state trajectories, was found to have a peak centered at 5.5 Å, which is fairly close to the experimental O_{5r}−N distance of 4.87 Å.[9] In the excited state, even though the simulations were initiated from the same initial structure as in the ground state, the dominant peak shifts to 3.05 Å. Also, it is interesting to note that the *B* factor of the terminal N atom in Lys531 (∼24) is much larger than the average *B* factor of the entire protein (∼15),[9] suggesting that the side chain has a relatively high mobility.

Possibility of the Transfer of a Proton from Lys531 to Oxyluciferin. The readily formed ion pair with a protonated Lys group and the high proton affinity of O_{5r} may lead to a proton-transfer reaction between OLU^- and Lys in the excited state. In fact, such a direct excited state proton transfer (ESPT) has been known to proceed much faster (∼1.2 ps in an intramolecular manner[48] and ∼350 ps in an intermolecular manner[49]) than the usual luminescence lifetime. The water mediation effect for the transfer has also been widely studied for various systems.[50] Indeed, if such a transfer happens with OLU^-, it will open a catalysis channel for the formation of the phenolate−enol species and will support the recent proposal[14a] of its role as the light emitter. Moreover, the estimated excited state proton affinity of OLU^- on O_{5r} described above is even larger than the proton affinity of the Lys side chain (butylamine) in the gas phase. Even if the keto-to-enol tautomerization does not readily occur, as long as the proton can be transferred before the deexcitation of the excited state, the luminescence will commence from this new neutral species, and not from the nascent keto molecule.[47]

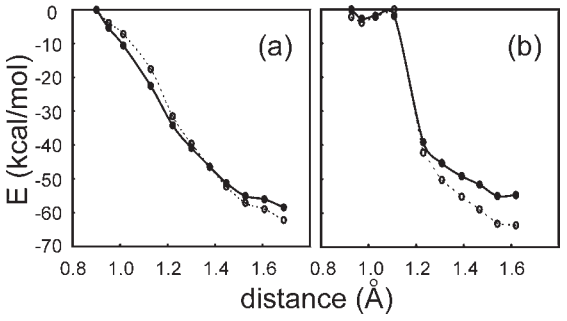

Figure 4. Energetics of hypothetical proton-transfer reactions from Lys531 to oxyluciferin in the excited state obtained with the QM/MM method in the (a) direct and (b) bridged ion pair cases. The solid lines represent RI-CIS(D)/MM surfaces, while the dotted lines show SA-CASSCF(8,8)/MM results. The horizontal axis shows the lysine proton−acceptor oxygen distance, which should be around 1 Å after the completion of the hypothetical proton transfer. In the SA-CASSCF calculations, inactive orbitals were frozen as Hartree−Fock orbitals for computational efficiency. The energy curves were vertically shifted arbitrarily for the sake of visual clarity.

However, because of the stabilizing solvation effect caused by the surroundings, the above-mentioned gas phase data will not be relevant in explaining the actual energetics in the condensed phase. For example, it is not likely that the pK_a of OLUH* would be as large as ∼10, the pK_a of the primary amine group in Lys. Namely, under the bulk aqueous condition, OLU^{-*} will potentially have a lower proton affinity than Lys. Because the physiological condition is somewhere between the gas phase and the aqueous state, this possibility of proton transfer needs to be more carefully assessed. Even in the gas phase, OLU^{-*} and $LysH^+$ in the vicinity can be stabilized by Coulombic interaction, and the proton affinity difference calculated with infinitely separated OLU^{-*} and Lys may be inadequate for understanding the complete picture.

To check this possibility of ESPT, we have performed the constrained QM/MM geometry optimizations to obtain the potential energy profile along the proton-transfer coordinate. In this calculation, the QM region includes OLU^-, Lys531, and the nearest water molecule around O_{5r}. We set the distance between the transferrable proton on Lys531 (donor) and its hydrogen-bonded O_{5r} (acceptor) constrained. The results are presented in Figure 4 for both direct and bridged cases. These results show that the proton-transfer reaction is energetically not feasible in the condensed phase regardless of whether it is mediated by water. Interestingly, in the bridged case in the gas phase, the proton transfer appears to be energetically feasible (Figure S1 of the Supporting Information). This is mainly due to the Coulombic destabilization in the ion pair (proton untrasferred state), where

the negative (OLU^-) and positive ($LysH^+$) charges are separated by a large distance. In the condensed phase, however, the solvation by water and/or protein groups effectively stabilizes the separated charges in this proton-untransferred state. In any case, ESPT from $LysH^+$ to OLU^- is an unlikely event even in the excited state. Thus, we can see that the formation of enol will not be facilitated through a catalytic proton-transfer route from the adjacent Lys group.[51]

The reasoning described above is further supported by an energy comparison between the enol−OLU^- and keto−OLU^- species. According to the work of Yang and Goddard[42] and Lindh and co-workers[14b] with CASPT2 calculations, the energy gap between the two species is 16−18 kcal/mol in the gas phase (keto being more stable). We have found a comparable gap of ∼13 kcal/mol after a quick calculation with EOM-CCSD/6-31+G(d) at the SOS-CIS(D_0)/6-31+G(d) geometries.[26] Even though enol-OLU^- can be stabilized over keto-OLU^- in protein by 3.35 kcal/mol through a hydrogen bond with the phosphate group in AMP as reported by Lindh and co-workers with QM(MS-CASPT2/CASSCF)/MM calculations,[14b] the energy difference is rather small, and thus, the ordering might even reverse if the hydrogen bond between keto-OLU^- and Lys531 is additionally considered. Therefore, with the lack of a catalytic protonation path explained above, we deduce that the nascent OLU^-* (keto form) as computationally supported by Morokuma and co-workers[12g] and by Lindh and co-workers[21] will not convert to enol within the lifetime of the excited state.

Effect of the Surroundings on Oxyluciferin Emission. If the keto form is the single species that can exist within the lifetime of the nascent excited state, what will be the driving force for generating various colors in different species? In answering this question, we need to consider one important characteristic of OLU^-, the distribution of the negative charge within the molecule. Because of the large electronegativity of oxygen, not surprisingly, the negative charge is concentrated on the two oxygen atoms (O_{5r} and O_{6r}). Interestingly, the $S_0 \leftrightarrow S_1$ transition involves a significant amount of charge transfer, and the negative charge populations on the two atoms change to large extents after the electronic transition. In fact, O_{5r} becomes more negative in the excited state by 0.137 *e* compared to the ground state.[26] In a condensed phase, this difference will of course induce changes in the surrounding structure as explained in a previous section, and such structural variation will be linked to the emission color change like the well-known solvatochromic shift.[52]

Indeed, such a shift is clearly seen in Figure 5, which compares the distributions of OLU^- emission energies simulated with the previously explained QM/MM scheme at conformations obtained from the excited state MD trajectories with and without surrounding protein and water molecules. The spectral diversity in the protein/water-stripped ensemble reflects the extent to which the emission energy changes due to geometrical fluctuations of OLU^-. The spectral diversity in the ensemble with protein and water shows the additional emission energy changes from the surrounding effect. From this figure, two aspects are obvious. With the surrounding molecules, the spectrum shifts to the red side and, at the same time, the emission becomes broader. In fact, the broadening, when measured by the half-width at half-maximum of the fitted Gaussian curve for the condensed phase data, amounts to 0.15 eV. This is comparable to the energy difference between red and green emissions in fireflies. For example, the 0.16 eV difference was observed between red and yellow emissions from the Japanese firefly (*Luciola cruciata*).[9]

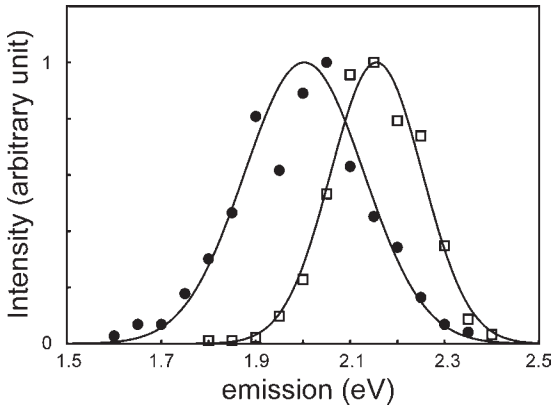

Figure 5. QM/MM simulated oxyluciferin emission curves with (●) and without (□) the surrounding protein and water. In both cases, the oxyluciferin structures were obtained from excited state simulations with protein and water.

One potential explanation for this broadening effect is the diversity of water coordination around OLU^-. For example, because more negative charge resides on O_{5r} in the excited state than in the ground state, when the O_{5r} side is more solvated by water than the O_{6r} side, the excited state will be more stabilized than the ground state (red shift). Likewise, more water on the O_{6r} side will shift the emission to the blue. To verify this proposition, we have grouped the conformations with respect to the number difference in coordinating water molecules (Δw) on the two oxygen atoms.[26] When $\Delta w = 1$ (one more H_2O on O_{5r}), $\Delta w = 0$, and $\Delta w = -1$ (one more H_2O on O_{6r}), the average emission energies with RI-CIS(D) without EOM-CCSD corrections were found to be 1.419, 1.429, and 1.449 eV, respectively. Thus, as expected, stronger water coordination around O_{5r} stabilizes the excited state more than the ground state. This is also in qualitative agreement with the multicolor bioluminescence results of Lindh and co-workers depending on the polarization of the surroundings (e.g., external electrostatic potential).[12d] However, the difference described above (∼0.03 eV at most) is almost negligibly small. Moreover, with different criteria for obtaining Δw, this weak dependence sometimes even disappeared. Thus, we should consider that the water solvation effect is not a crucial factor for broadening the emission energy distribution. As a matter of fact, even when the S_0-S_1 gap is calculated as a function of intermolecular distance for the OLU−water heterodimer in the gas phase, the gap does not depend that strongly on the distance unless the two molecules are very close. Namely, the hydrogen bond between OLU^- and water has an only limited effect on the emission modification.

However, because of the long-range (the $O_{5r}-O_{6r}$ distance is 10.5 Å in the stable geometry) charge-transfer character between S_0 and S_1, and the subsequent large transition dipole moment, a strong correlation between the electric field vector exerted on OLU^- and the S_0-S_1 gap is anticipated. To substantiate this, we have inspected the dependence of the QM/MM emission energy with respect to the difference in the electrostatic potentials (ESPs) at the O_{5r} and O_{6r} positions. This ESP (Ψ) difference will of course well represent the electric field exerted on the OLU^- molecule. From Figure 6, we can see that the emission energy changes in clear accordance with the ESP difference. In addition, the trend is in exact agreement with our anticipation: a lower ESP on O_{5r} will destabilize OLU^-, and because this

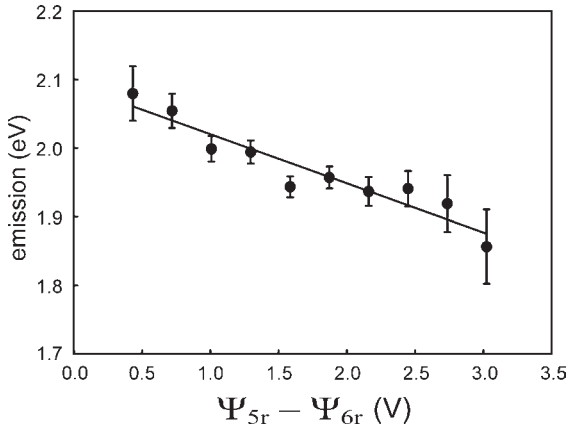

Figure 6. Correlation between the QM/MM emission energy and the ESP difference on O_{5r} and O_{6r}. The ESPs were calculated by considering all MM particles.

destabilization is larger in the excited state with a larger negative charge on O_{5r}, the emission will be on the bluer side with a lower Ψ_{5r}. Likewise, a higher ESP on O_{6r} will lead to a greater stabilization in the ground state with a larger negative charge on the atom and will also have a blue shift effect on the emission. Thus, the smaller value of $\Psi_{5r} - \Psi_{6r}$ will yield bluer emission, which is exactly observed in Figure 6. Interestingly, this ESP effect has an overall spectral shift (or broadening) amounting to ~0.2 eV, which is the emission color span of OLU^- bound to different luciferases. Thus, we can infer that the color variation of OLU bioluminescence is in fact closely related to the ESP modulation from the dynamic fluctuation of the protein complex.

Finally, to investigate which group is most responsible for this variation, we have tried different combinations of protein side chains and ligand groups for the consideration of the ESP effect. Among various possible combinations, the role of the neighboring Lys531 (formally with a +1 charge) and AMP (formally with a −2 charge) groups was most noticeable. As shown in Figure 7a, the emission energies versus ESP differences calculated only with these two groups exhibit a similar trend. Moreover, most of the trend can be recovered with the ESP value on O_{5r} only (Figure 7b). Thus, we can additionally infer that these two charged residues are the dominating factor for deciding the emission character at least in the firefly luciferase considered in this work. These results are in good accord with the work of Lindh and co-workers, which showed similar correlations between the emission energy and the ESP on O_{5r} from the AMP group based on excited state calculations at six different model conformations.[12d] Interestingly, other nearby charged residues such as Arg220, Glu313, and Arg339, which are closer to O_{6r} than O_{5r}, were found to have a similar effect but to a much lesser extent. The reason for this reduced effect is the different degrees of structural freedom. These residues move much less freely at a larger distance in space (for example, the terminal C atom in Arg339 is 7.9 Å from O_{6r}), and the range of ESP values exerted on O_{6r} from these residues is ~3 times smaller than the ESP range on O_{5r} from Lys531 and AMP (Figure S2 of the Supporting Information). This situation may surely change with different luciferases, and in this sense, it is not surprising to see various different emission colors from different luciferases. For example, the crystal structures of green- and red-emitting luciferases show an ~25% different Arg339 flexibility when judged by its *B* factor.[9]

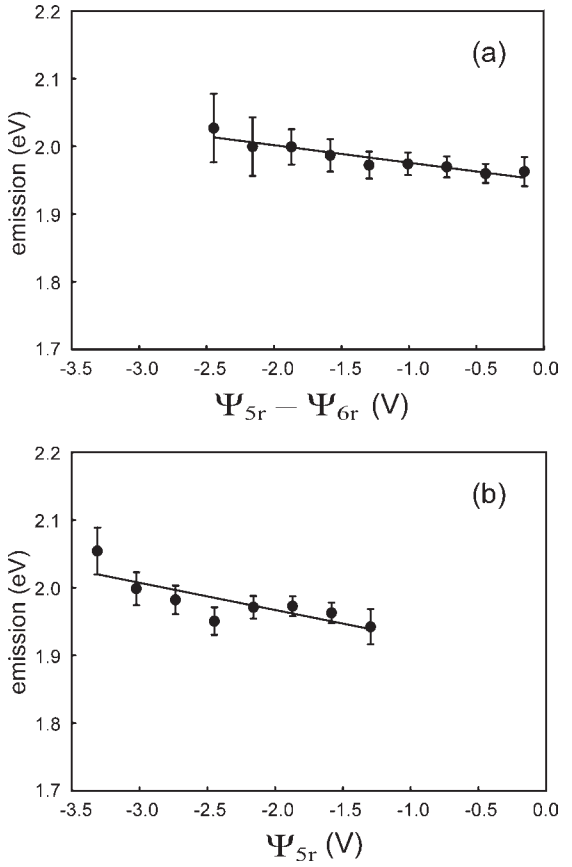

Figure 7. Correlation between the QM/MM emission energy and the ESPs from Lys531 and AMP residues.

Thus, it will be interesting to study how the dynamic residue flexibility will affect the overall emission profiles for different enzymes. We hope to report on this as a continuation of this work.

In short, we can see that the motions of the surrounding groups such as water, cofactors (AMP in this case), and the enzyme itself can induce a spectral shift and broadening of emission. Among these groups, charged ones are definitely important in tuning the emission characters, especially for chromophores with charge-transfer transitions, and the mobility of the surrounding group very significantly affects the emission. The solvation effect of water is less significant, however, compared to the electric field variation at least in the case of OLU^-. Of course, the situation may change depending on the character of the luminophore. Also, residues that can move relatively freely within the lifetime of the luminescing ligand will play a more important role in modulating the emission color.

4. CONCLUSION

We have used various theoretical approaches to reveal the fundamental nature of bioluminescence in the firefly luciferase−oxyluciferin complex, on the basis of a model we have developed[26] for describing the physiological emission condition as closely as possible. Most importantly, in our analysis, we have employed dynamic features in both the electronic ground and excited states, which may not be easily accessed by experimental means. Through this, we have shown that local structure around the luminophore in the excited state is quite different from the ground state case, mainly because of the strong charge-transfer character involved with the electronic transition of the luminophore.

We believe this will likely be generally true in biological systems with electronic transitions, where charge transfer is widely found in relation to photon absorption or emission.

In fact, structural reorganizations upon charge-transfer transitions of solute molecules with polar solvents have been extensively studied,[53] and the same principle is now applied to understanding the behavior of biological systems.[54] Specifically with respect to oxyluciferin, we have shown that the solvation dynamics on the two ends of the molecule is markedly different when bound in the protein. On its thiazole side, where the water solvation is not effective, a protonated protein side chain (Lys531) takes an important role in stabilizing the large negative partial charge of the chromophore in the excited state. This promotes the formation of an ion pair between Lys531 and the chromophore, which is dominant regardless of the water content around oxyluciferin. Formation of the pair is possible because Lys531 is flexible. The hypothetical transfer of a proton from Lys531 to oxyluciferin is shown to be unfeasible on the basis of its energetics. Thus, the keto-to-enol transformation is not likely, and the keto form will be the only emitting species. The structural fluctuations of flexible charged groups can instead modulate the emission color over a wide spectral range through electrostatic interactions. We believe new experiments such as point mutations on the strongly interacting residues and time-resolved spectroscopic measurements on the residue−oxyluciferin interactions after electronic transitions can be further designed to verify our theoretical predictions and to improve our understanding of the interesting phenomena around bioluminescence.

Finally, we stress that dynamical features on the excited state surface should always be considered in properly characterizing bioluminescent systems. As we have shown in this work, the emitting molecule possesses very different electron distributions before and after emitting a photon, which induces different surrounding structure and interacting patterns with the protein. This structural and dynamical information may not be drawn fully adequately from ground state-based experimental methods. Also, because the excited state has a finite and relatively short lifetime, the feasibility of any reaction on the excited state surface should be examined within such time scales through dynamical studies. In the oxyluciferin case, for example, the debated keto versus enol identity should be considered by inspecting the feasibility of the isomerization within the time scale of the emission. Of course, dynamical studies as we have presented here will be very useful for such considerations, and combination of theoretical approaches with experiments will be extremely important for understanding similar systems.

■ ASSOCIATED CONTENT

Ⓢ Supporting Information. Complete citations of refs 32 and 33; free space volumes around the two terminal oxygen atoms of oxyluciferin (Table S1), excited state proton-transfer energetics from Lys531 to oxyluciferin in the gas phase, electrostatic potential effect exerted by charged residues around benzothiazole oxygen, Figures S1−S3, and coordinates and absolute energies of HOLU, OLU^-, and OLUH. This material is available free of charge via the Internet at http://pubs.acs.org.

■ AUTHOR INFORMATION

Corresponding Author
ymrhee@postech.ac.kr

■ ACKNOWLEDGMENT

This work was supported by the WCU Program (Grant R32-2008-000-10180-0) and the Basic Science Research Program (Grant 2009-0067085) through the National Research Foundation of Korea (NRF) funded by the Ministry of Education, Science, and Technology. The supercomputer time from the Korea Institute of Science and Technology Information via Grant KSC-2011-C2-09 is also gratefully acknowledged.

■ REFERENCES

(1) McCapra, F. *Acc. Chem. Res.* **1976**, *9*, 201–208.
(2) Biggley, W. H.; Lloyd, J. E.; Seliger, H. H. *J. Gen. Physiol.* **1967**, *50*, 1681–1692.
(3) (a) Seliger, H. H.; McElroy, W. D. *Arch. Biochem. Biophys.* **1960**, *88*, 136–141. (b) Ando, Y.; Niwa, K.; Yamada, N.; Enomoto, T.; Irie, T.; Kubota, H.; Ohmiya, Y.; Akiyama, H. *Nat. Photonics* **2007**, *2*, 44–47.
(4) McElroy, W. D.; DeLuca, M. A. *J. Appl. Biochem.* **1983**, *5*, 197–209.
(5) White, E. H.; Rapaport, E.; Seliger, H. H.; Hopkins, T. A. *Bioorg. Chem.* **1971**, *1*, 91–122.
(6) Morton, R. A.; Hopkins, T. A.; Seliger, H. H. *Biochemistry* **1969**, *8*, 1598–1607.
(7) McCapra, F.; Gilfoyle, D. J.; Young, D. W.; Church, N. J.; Spencer, P.; Campbell, A. K.; Kricka, L. J.; Stanley, P. E. *Bioluminescence and Chemiluminescence: Fundamental and Applied Aspects*; John Wiley and Sons: Chichester, U.K., 1994.
(8) Branchini, B. R.; Southworth, T. L.; Murtiashaw, M. H.; Magyar, R. A.; Gonzalez, S. A.; Ruggiero, M. C.; Stroh, J. G. *Biochemistry* **2004**, *43*, 7255–7262.
(9) Nakatsu, T.; Ichiyama, S.; Hiratake, J.; Saldanha, A.; Kobashi, N.; Sakata, K.; Kato, H. *Nature* **2006**, *440*, 372–376.
(10) (a) Gross, S.; Piwnica-Worms, D. *Nat. Methods* **2005**, *2*, 607–614. (b) Sheikh, A. Y.; Lin, S. A.; Cao, F.; Cao, Y.; van der Bogt, K. E.; Chu, P.; Chang, C. P.; Contag, C. H.; Robbins, R. C.; Wu, J. C. *Stem Cells* **2007**, *25*, 2677–2684.
(11) (a) Theodossiou, T.; Hothersall, J. S.; Woods, E. A.; Okkenhaug, K.; Jacobson, J.; MacRobert, A. J. *Cancer Res.* **2003**, *63*, 1818–1821. (b) Schipper, M. L.; Patel, M. R.; Gambhir, S. S. *Mol. Imaging Biol.* **2006**, *8*, 218–225.
(12) (a) Milne, B. F.; Marques, M. A.; Nogueira, F. *Phys. Chem. Chem. Phys.* **2010**, *12*, 14285–14293. (b) Naumov, P.; Kochunnoonny, M. *J. Am. Chem. Soc.* **2010**, *132*, 11566–11579. (c) Min, C. G.; Ren, A. M.; Guo, J. F.; Zou, L. Y.; Goddard, J. D.; Sun, C. C. *ChemPhysChem* **2010**, *11*, 2199–2204. (d) Navizet, I.; Liu, Y. J.; Ferre, N.; Xiao, H. Y.; Fang, W. H.; Lindh, R. *J. Am. Chem. Soc.* **2010**, *132*, 706–712. (e) Tagami, A.; Ishibashi, N.; Kato, D.; Taguchi, N.; Mochizuki, Y.; Watanabe, H.; Ito, M.; Tanaka, S. *Chem. Phys. Lett.* **2009**, *472*, 118–123. (f) Hirano, T.; Hasumi, Y.; Ohtsuka, K.; Maki, S.; Niwa, H.; Yamaji, M.; Hashizume, D. *J. Am. Chem. Soc.* **2009**, *131*, 2385–2396. (g) Chung, L. W.; Hayashi, S.; Lundberg, M.; Nakatsu, T.; Kato, H.; Morokuma, K. *J. Am. Chem. Soc.* **2008**, *130*, 12880–12881. (h) Liu, Y. J.; De Vico, L.; Lindh, R. *J. Photochem. Photobiol. A* **2008**, *194*, 261–267. (i) Pinto da Silva, L.; Esteves da Silva, J. C. G. *J. Chem. Theory Comput.* **2011**, *7*, 809–817.
(13) (a) White, E. H.; Roswell, D. F. *Photochem. Photobiol.* **1991**, *53*, 131–136. (b) Dahlke, E. E.; Cramer, C. J. *J. Phys. Org. Chem.* **2003**, *16*, 336–347.
(14) (a) Naumov, P.; Ozawa, Y.; Ohkubo, K.; Fukuzumi, S. *J. Am. Chem. Soc.* **2009**, *131*, 11590–11605. (b) Chen, S. F.; Liu, Y. J.; Navizet, I.; Ferre, N.; Fang, W. H.; Lindh, R. *J. Chem. Theory Comput.* **2011**, *7*, 798–803.
(15) (a) Granucci, G.; Hynes, J. T.; Millie, P.; Tran-Thi, T. H. *J. Am. Chem. Soc.* **2000**, *122*, 12243–12253. (b) Webb, S. P.; Yeh, S. W.; Philips, L. A.; Tolbert, M. A.; Clark, J. H. *J. Am. Chem. Soc.* **1984**, *106*, 7286–7288.
(16) (a) Isobe, H.; Takano, Y.; Okumura, M.; Kuramitsu, S.; Yamaguchi, K. *J. Am. Chem. Soc.* **2005**, *127*, 8667–8679. (b) Liu, F. Y.; Liu, Y. J.; De Vico, L.; Lindh, R. *Chem. Phys. Lett.* **2009**, *484*, 69–75.

(17) Shimomura, O.; Goto, T.; Johnson, F. H. *Proc. Natl. Acad. Sci. U.S.A.* **1977**, *74*, 2799–2802.
(18) Branchini, B. R.; Murtiashaw, M. H.; Magyar, R. A.; Portier, N. C.; Ruggiero, M. C.; Stroh, J. G. *J. Am. Chem. Soc.* **2002**, *124*, 2112–2113.
(19) Orlova, G.; Goddard, J. D.; Brovko, L. Y. *J. Am. Chem. Soc.* **2003**, *125*, 6962–6971.
(20) Li, Z. W.; Ren, A. M.; Guo, J. F.; Yang, T.; Goddard, J. D.; Feng, J. K. *J. Phys. Chem. A* **2008**, *112*, 9796–9800.
(21) Liu, F.; Liu, Y.; De Vico, L.; Lindh, R. *J. Am. Chem. Soc.* **2009**, *131*, 6181–6188.
(22) KrishnaMurthy, N. V.; Sudhaharan, T.; Reddy, A. R. *Spectrochim. Acta, Part A* **2007**, *68*, 851–859.
(23) Here, a physiological condition means a situation in which OLU, luciferase, and charge-neutralizing counterions are present and the temperature and pressure are set to ambient conditions.
(24) Hess, B.; Kutzner, C.; van der Spoel, D.; Lindahl, E. *J. Chem. Theory Comput.* **2008**, *4*, 435–447.
(25) "OLU^-" is equivalent to the more conventional notation "phenolate-keto-OxyLH^-". We will adopt this nonconventional notation as it simplifies our later discussion regarding its protonated states.
(26) Song, C.-I.; Rhee, Y. M. *Int. J. Quantum Chem.*, in press, DOI 10.1002/qua.22957.
(27) Park, J. W.; Kim, H. W.; Song, C.-I.; Rhee, Y. M. *J. Chem. Phys.* **2011**, *135*, 014107.
(28) Weiner, S. J.; Kollman, P. A.; Nguyen, D. T.; Case, D. A. *J. Comput. Chem.* **1986**, *7*, 230–252.
(29) Jorgensen, W. L.; Tirado-Rives, J. *J. Am. Chem. Soc.* **1988**, *110*, 1657–1666.
(30) Berendsen, H. J. C.; Postma, J. P. M.; Gunsteren, W. F. v.; DiNola, A.; Haak, J. R. *J. Chem. Phys.* **1984**, *81*, 3684–3690.
(31) Hess, B.; Bekker, H.; Berendsen, H. J. C.; Fraaije, J. G. E. M. *J. Comput. Chem.* **1997**, *18*, 1463–1472.
(32) Shao, Y.; et al. *Phys. Chem. Chem. Phys.* **2006**, *8*, 3172–3191.
(33) Brooks, B. R.; et al. *J. Comput. Chem.* **2009**, *30*, 1545–1614.
(34) Foresman, J. B.; Head-Gordon, M.; Pople, J. A.; Frisch, M. J. *J. Phys. Chem.* **1992**, *96*, 135–149.
(35) (a) Head-Gordon, M.; Rico, R. J.; Oumi, M.; Lee, T. J. *Chem. Phys. Lett.* **1994**, *219*, 21–29. (b) Rhee, Y. M.; Head-Gordon, M. *J. Phys. Chem. A* **2007**, *111*, 5314–5326.
(36) (a) Roos, B. O.; Taylor, P. R.; Siegbahn, P. E. M. *Chem. Phys.* **1980**, *48*, 157–173. (b) Werner, H. J.; Knowles, P. J. *J. Chem. Phys.* **1985**, *82*, 5053–5063. (c) Knowles, P. J.; Werner, H. J. *Chem. Phys. Lett.* **1985**, *115*, 259–267.
(37) Dreuw, A.; Head-Gordon, M. *J. Am. Chem. Soc.* **2004**, *126*, 4007–4016.
(38) (a) Rhee, Y. M.; Lee, T. J.; Gudipati, M. S.; Allamandola, L. J.; Head-Gordon, M. *Proc. Natl. Acad. Sci. U.S.A.* **2007**, *104*, 5274–5278. (b) Curtiss, L. A.; Raghavachari, K.; Redfern, P. C.; Rassolov, V.; Pople, J. A. *J. Chem. Phys.* **1998**, *109*, 7764–7776.
(39) Senn, H. M.; Thiel, W. *Angew. Chem., Int. Ed.* **2009**, *48*, 1198–1229.
(40) Roos, B. O.; Lindh, R.; Malmqvist, P. A.; Veryazov, V.; Widmark, P. O. *J. Phys. Chem. A* **2004**, *108*, 2851–2858.
(41) Finley, J.; Malmqvist, P. A.; Roos, B. O.; Serrano-Andres, L. *Chem. Phys. Lett.* **1998**, *288*, 299–306.
(42) Yang, T.; Goddard, J. D. *J. Phys. Chem. A* **2007**, *111*, 4489–4497.
(43) Werner, H. J. *Mol. Phys.* **1996**, *89*, 645–661.
(44) Roos, B. O.; Andersson, K. *Chem. Phys. Lett.* **1995**, *245*, 215–223.
(45) Werner, H.-J.; Knowles, P. J.; Lindh, R.; Manby, F. R.; Schütz, M. *MOLPRO*, version 2009.1; 2009 (a package of ab initio programs; see http://www.molpro.net).
(46) OLUH is a protonated keto species and should not be confused with enol.
(47) Min, C. G.; Ren, A. M.; Guo, J. F.; Li, Z. W.; Zou, L. Y.; Goddard, J. D.; Feng, J. K. *ChemPhysChem* **2010**, *11*, 251–259.
(48) Kim, C. H.; Park, J.; Seo, J.; Park, S. Y.; Joo, T. *J. Phys. Chem. A* **2010**, *114*, 5618–5629.
(49) Toh, K. C.; Stojkovic, E. A.; van Stokkum, I. H.; Moffat, K.; Kennis, J. T. *Proc. Natl. Acad. Sci. U.S.A.* **2010**, *107*, 9170–9175.
(50) (a) Syage, J. A.; Steadman, J. *J. Chem. Phys.* **1991**, *95*, 2497–2510. (b) Kaneko, S.; Yotoriyama, S.; Koda, H.; Tobita, S. *J. Phys. Chem. A* **2009**, *113*, 3021–3028. (c) Gaigeot, M. P.; Cimas, A.; Seydou, M.; Kim, J. Y.; Lee, S.; Schermann, J. P. *J. Am. Chem. Soc.* **2010**, *132*, 18067–18077.
(51) It will be more desirable to use a prohibitively expensive multireference-based method for generating structures for the energy profiles in Figure 4, especially because the single-reference description will be prone to errors around the conformation with a "half-migrated" proton. However, two stable sides of the potential profile (OLU^-/$LysH^+$ and OLUH/Lys) can be described well within the single-reference regime, and comparison of the energies of the two sides can still be obtained reliably with our more practical approach. See: Coe, J. D.; Levine, B. G.; Martinez, T. J. *J. Phys. Chem. A* **2007**, *111*, 11302–11310. Aquino, A. J.; Barbatti, M.; Lischka, H. *ChemPhysChem* **2006**, *7*, 2089–2096.
(52) Suppan, P. *J. Photochem. Photobiol. A* **1990**, *50*, 293–330.
(53) Fleming, G. R.; Cho, M. H. *Annu. Rev. Phys. Chem.* **1996**, *47*, 109–134.
(54) (a) Furse, K. E.; Corcelli, S. A. *J. Am. Chem. Soc.* **2008**, *130*, 13103–13109. (b) Furse, K. E.; Corcelli, S. A. *J. Phys. Chem. Lett.* **2010**, *1*, 1813–1820.